minerals

MDPI

Article

Injection of a CO_2-Reactive Solution for Wellbore Annulus Leakage Remediation

Laura Wasch * and Mariëlle Koenen

TNO, Princetonlaan 6, 3584 CB Utrecht, The Netherlands; marielle.koenen@tno.nl

* Correspondence: laura.wasch@tno.nl; Tel.: +31-64966157

Received: 31 July 2019; Accepted: 16 October 2019; Published: 22 October 2019

Abstract: Driven by concerns for safe storage of CO_2, substantial effort has been directed on wellbore integrity simulations over the last decade. Since large scale demonstrations of CO_2 storage are planned for the near-future, numerical tools predicting wellbore integrity at field scale are essential to capture the processes of potential leakage and assist in designing leakage mitigation measures. Following this need, we developed a field-scale wellbore model incorporating (1) a de-bonded interface between cement and rock, (2) buoyancy/pressure driven (microannulus) flow of brine and CO_2, (3) CO_2 diffusion and reactivity with cement and (4) chemical cement-rock interaction. The model is aimed at predicting leakage through the microannulus and specifically at assessing methods for CO_2 leakage remediation. The simulations show that for a low enough initial leakage rate, CO_2 leakage is self-limiting due to natural sealing of the microannulus by mineral precipitation. With a high leakage rate, CO_2 leakage results in progressive cement leaching. In case of sustained leakage, a CO_2 reactive solution can be injected in the microannulus to induce calcite precipitation and block the leak path. The simulations showed full clogging of the leak path and increased sealing with time after remediation, indicating the robustness of the leakage remediation by mineral precipitation.

Keywords: CO_2 leakage; cement; well integrity; leakage remediation; TOUGHREACT; reactive transport modelling

1. Introduction

Large scale geological storage of CO_2 can significantly reduce CO_2 emissions and limit global warming [1]. Geological reservoirs are selected for the physical containment of CO_2 which guarantees permanent storage in the subsurface. However, CO_2 injection wells (and possibly old oil and gas wells) penetrating the reservoirs and the caprocks above can compromise the integrity of the storage complex. Wells have a primary structural seal of casing and annular cement (between the casing and the geological formation) and a cement plug when abandoned. Despite these seals, many oil and gas wells leak during their operational lifetime or after abandonment through leakage pathways formed by cement shrinkage or pressure and temperature fluctuations [1]. If annular cement is placed properly, the most likely leak path for CO_2 is along the well through fractures in the cement or microannuli between the cement and the casing or adjacent rock [2–5].

CO_2 leakage through microannuli will cause dissolution of CO_2 in the pore waters which acidifies the near-wellbore environment and causes cement reactivity. Reactions of cement in contact with CO_2-rich water or brine have been extensively studied with experiments and by numerical modelling [6–13]. A typical wellbore cement mineralogy consists of mainly portlandite ($Ca(OH)_2$) and calcium silicate hydrate (CSH), with minor phases such as aluminium-, iron-, magnesium-, or calcium-containing sulphate-, carbonate-, or silicate-hydrates [14]. In general, cement-CO_2 interaction is primarily characterized by portlandite dissolution and subsequent precipitation of calcium carbonate ($CaCO_3$) because of the fast reaction kinetics. The dissolving CSH phase forms additional calcium

carbonate and amorphous silica gel (SiO_2) [7]. Characteristic successive, inward moving reaction zones are observed consisting of portlandite dissolution, calcite precipitation, and subsequent calcite dissolution from the rim, leaving a porous, silica-rich rim [6,10–12]. However, cement reactivity will most-likely only lead to cement degradation under leaching/flow conditions when reaction products are quickly removed from the reaction site. At no/low flow conditions, calcite precipitation is the dominant process rather than (re-)dissolution [4,15,16]. Depending on the initial flow and chemical conditions, continuous cement leaching occurs, or cement reactivity may actually support natural sealing of the micro annulus [17–19].

In the case of sustained CO_2 leakage, a corrective measures plan must be in place and appropriate remediation measures should be taken [20,21]. Intentional clogging of the near-well area with salt has been proposed as a preventative measure against CO_2 leakage [22]. This method was based on the capacity of injected CO_2 to evaporate water and precipitate pore filling salt. The process of natural sealing of the microannulus by mineral precipitation indicates a potential for chemical clogging of the annulus leak path. Clogging with calcite or silica has already been proposed for a CO_2 leak path through the caprock [23–25]. To induce mineralization in a leak path, it was proposed to inject a silica- or calcium-rich suspension or solution into the CO_2-containing environment. The injected solution will react in the acid environment to form a solid silica (gel) or carbonate mineral. A modelling study on leakage remediation above a leaking fault through a caprock indicated a final leakage reduction of up to 95% [25]. Experimental [23] and modelling results [24,25] for caprock leakage mitigation support the feasibility of the method for reactive clogging by injecting a CO_2-reactive solution into a high permeable leak path to form solid reactants that clog the leak path, reduce permeability and stop leakage. The main objective of this study is to assess the possibility of reactive leakage mitigation for wellbore annulus leakage.

We developed a field scale reactive transport model based on the model reported by Koenen and Wasch [18] to simulate CO_2 leakage through a microannulus, resulting in either sustained flow and cement leaching or in natural sealing and reduced leakage. For the leakage cases, we study the potential of induced CO_2 mineralization in the leak path, mitigating CO_2 leakage. The numerical modelling study includes the following processes:

- Flow of supercritical CO_2 and brine along the initially water-saturated microannulus;
- Diffusion of dissolved CO_2 into the caprock;
- Diffusion of dissolved CO_2 into impermeable cement and reactions of dissolved CO_2 and cement;
- Leakage into the aquifer overlying the caprock;
- Injection of a CO_2-reactive solution in the microannulus leak path to promote clogging by calcite formation;

In this paper, we report on microannulus leakage (versus sealing), the intentional clogging process for leakage remediation, and the post-clogging phase to assess the sustainability of the clogging procedure.

2. Materials and Methods

A reactive transport model was developed in TOUGHREACT (Version 3, Lawrence Berkeley National Laboratory, Oakland, CA, USA) [26], a simulator for coupled modelling of multiphase fluid and heat flow, solute transport, and chemical reactions by introducing reactive transport into the flow simulator TOUGH2. We use the ECO2N fluid property module to include the thermodynamic and thermophysical properties of H_2O–NaCl–CO_2 mixtures [27].

A 2D axisymmetric field-scale model (Figure 1) was adapted from the model reported in [18]. The well consists of two cemented casings: a 9 5/8″ casing of 3590 m depth into the reservoir and a 13 3/8″ casing to a depth of 2569 m. We assume a 0.5 cm thick casing (unreactive transport barrier) and a 3 cm thick annular cement. A 500-micron thick, porous and highly permeable micro-annulus is defined between the cement and the adjacent rock. For the rock formations, three layers are defined: a reservoir

(infinite volume, representing a large storage reservoir), an impermeable caprock (550 m thick) and an overlying, permeable aquifer (3040 m thick). Simulations are performed in isothermal mode, with a (fixed) temperature gradient from reservoir to surface. To reduce simulation times, the upper 2500 m of the aquifer to the surface are removed after initializing pressure and temperature. The resulting mesh contains 70 layers and 36 columns. Vertical mesh refinement is defined around the layer interfaces and at the leakage remediation interval down to 5 cm. The mesh is refined towards the well in the radial direction, down to cells of 0.5 cm width for the annular cement. The pressure is equilibrated with depth; 25 °C and 1.5 bar at the top and 90 °C and 327 bar at reservoir level. This yields a 1180 m thick model with a radius of 150 m (Figure 1). The boundary conditions are represented by the infinite volume reservoir with a 0.8 CO_2 saturation and an infinite volume upper boundary for the microannulus. The reservoir was given a 20 bar overpressure to simulate upward leakage out of the CO_2 reservoir.

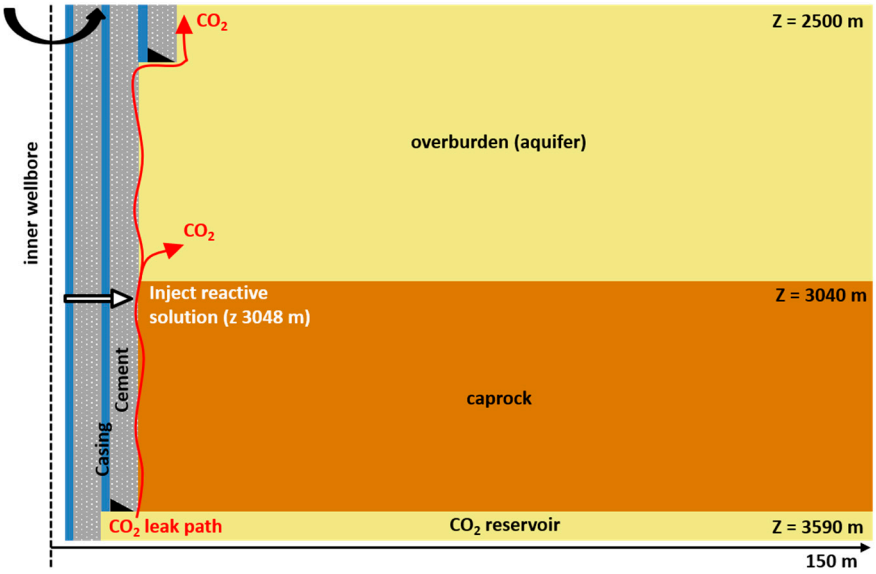

Figure 1. Schematic overview of the 2D radial symmetric TOUGHREACT model showing: the model dimensions, the different rock formations, the well and the leak path through the wellbore microannulus, and the location of leakage remediation.

The TOUGHREACT software is developed to simulate reactive transport through porous media and does not allow open space. Therefore, we defined the microannulus as cement material with a 0.9 volume fraction porosity, with the remaining 0.1 volume fraction made up by cement mineralogy. The 500-micron microannulus hence has an effective thickness of 450 micron, but the width of the microannulus may increase by 10% in case of cement mineral dissolution. The microannulus width (aperture) can be related to its permeability by the cubic law. For an aperture of 500 micron the permeability would be 4.2×10^{-9} m^2 (~4200 Darcy), however, the actual hydraulic permeability will be lower as it is affected by many factors such as fracture wall roughness. To account for this, simulations have been previously run with various initial (hydraulic) permeability values between 5×10^{-13} m^2 (~500 mDarcy) and 8.3×10^{-10} m^2, covering values reported in literature [18]. For the present study we use a permeability range between 1×10^{-13} m^2 and 1×10^{-11} m^2 to capture the uncertainty and natural variation in microannulus flow. For the base case, a permeability of 1.3×10^{-12} m^2 is selected.

The flow properties of the different materials used in the model are summarized in Table 1. For relative permeability, we use the equation from Corey's curve with a residual liquid and gas saturation of 0.02 and 0.1. The diffusion coefficient is calculated in TOUGHREACT by multiplying a standard diffusion coefficient (1×10^{-9} m^2/s) by the tortuosity, porosity and liquid saturation. Hence the effective diffusion coefficient will change over time as the porosity and saturation develop due to fluid flow and mineral reactions.

Table 1. Transport properties of the different materials used in the model. * In TOUGHREACT a permeability of 1.0×10^{-30} m^2 represents impermeable material.

Transport Properties	Unit	Reservoir	Cement	Caprock	Microannulus	Aquifer
Porosity	φ (-)	0.2	0.3	0.1	0.9	0.2
Permeability	k (m^2)	2.0×10^{-13}	1.0×10^{-30} *	1.0×10^{-30} *	1.3×10^{-12}	2.0×10^{-13}
Tortuosity	τ (-)	0.4	0.01	0.05	0.4	0.4
Capillary Curve						
Van Genuchten	λ (-)	0.2	-	-	-	0.2
	S_{lr} (-)	0.1	-	-	-	0.1
	$1/P_0$ (-)	0.002	-	-	-	0.002
	P_0 (Pa)	1.0×10^8	-	-	-	1.0×10^8
	S_{ls} (-)	1	-	-	-	1
TRUST	P_0 (Pa)	-	1.0×10^6	1.0×10^6	-	-
	S_{lr} (-)	-	0.2	0.2	-	-
	η (-)	-	0.4	0.4	-	-
	P_e (Pa)	-	4.0×10^6	4.0×10^6	-	-

The cement consists of portlandite, CSH_1.6 (CSH of a 1.6 Ca/Si ratio), monosulfoaluminate and hydrotalcite (Table 2). The secondary minerals for cement are calcite, amorphous silica, anhydrite, dolomite and gibbsite. A clastic rock was included consisting of quartz, albite, microcline, kaolinite, anhydrite, dolomite and calcite. We used the thermodynamic database Thermoddem (version 1.10, 6 Jun 2017, BRGM, France) to model chemical reactions [28]. The reaction of minerals is kinetically controlled using a rate expression of Lasaga et al. [29]. Mineral kinetics are listed in Table 3. The specific surface area is assumed 0.98 m^2/kg, except for the C-S-H phases and clays for which a value of 100 m^2/kg is assumed. The CO_2-reactive solution to stimulate microannulus clogging is designed by equilibrating lime with a sodium chloride brine at surface conditions. The different fluid compositions are listed in Table 4.

Table 2. Initial mineralogy of cement and aquifer/caprock and possible secondary minerals.

Mineral-Formula	Cement (Volume Fraction)	Aquifer/Caprock (Volume Fraction)
Portlandite-($Ca(OH)_2$)	0.2	-
CSH(1.6)-($Ca_{1.60}SiO_{3.6}$:2.58H_2O)	0.6	-
Monosulfoaluminate-($Ca_4Al_2SO_{10}$:12H_2O)	0.1	-
Hydrotalcite-($Mg_4Al_2O_7$:10H_2O)	0.1	-
Quartz-(SiO_2)	-	0.7
Calcite-($CaCO_3$)	-	0.01
Amorphous silica-(SiO_2)	-	-
Anhydrite-($CaSO_4$)	-	0.01
Dolomite-($CaMg(CO_3)_2$)	-	0.01
Gibbsite-($Al(OH)_3$)	-	-
Microcline-($K(AlSi_3)O_8$)	-	0.1
Albite-($NaAlSi_3O_8$)	-	0.1
Kaolinite-($Al_2Si_2O_5(OH)_4$	-	0.07

Porosity changes due to water-rock reactions are calculated in TOUGHREACT using mineral molar volumes. Porosity change can be related to permeability change by porosity-permeability relations, but they contain highly uncertain and material specific input parameters [30]. The Verma–Pruess relation (Equation (1)) is an extension of a Power Law relation considering a critical porosity at which the permeability is assumed zero. This relation is often used for mineral precipitation processes given the high impact of the critical porosity on porosities decreasing during mineral precipitation, while the

relevance of critical porosity in the mathematical expression diminishes for porosities increasing during dissolution [30]. We used the porosity-permeability relationship of Verma and Pruess [31] and addressed the uncertainty of the input parameters by a sensitivity study. The base case values are a 0.80 critical porosity and a power law component of 6.

$$\frac{k}{k_i} = \left(\frac{\varphi - \varphi_c}{\varphi_i - \varphi_c}\right)^n \quad (1)$$

where k is the permeability, k_i the initial permeability, φ the porosity, φ_i the initial porosity, φ_c the critical porosity below which the permeability is assumed zero, and n is a power law exponent.

Table 3. Kinetic rate parameters (*[a] [32], *[b] [33] and *[c] [34]).

Mineral	Acid Mechanism			Neutral Mechanism		Carbonate/Base Mechanism		
	Log (k25 °C) (mol/m²/s)	ΔH (kJ/mol)	n	Log (k25 °C) (mol/m²/s)	ΔH (kJ/mol)	Log (k25 °C) (mol/m²/s)	ΔH (kJ/mol)	n
Portlandite *[c]	−3.10	75	0.6	−7.66	75	-	-	-
C1.6SH *[c]	−7.23	23	−0.28	-	-	-	-	-
Monosulf. *[b]	−3.09	74.9	0.6	−11.2	15	-	-	-
Hydrotal. *[b]	−7.23	15	0.28	−17.8	15	-	-	-
Quartz *[a]	−7.52	56.9	0.5	−4.55	56.9	-	-	-
Calcite *[a]	−0.30	14.4	1	−5.81	23.5	−3.48	35.4	1
Silica(am) *[a]	-	-	-	−9.42	49.8	-	-	-
Anhydrite *[a]	-	-	-	−3.19	14.3	-	-	-
Dolomite *[a]	−3.19	36.1	0.5	−7.53	52.2	−5.11	34.8	0.5
Gibbsite *[a]	−7.65	47.5	0.99	−11.5	61.2	−16.7	80.1	−0.78
Albite *[a]	−10.2	65	0.46	−12.6	69.8	−15.6	71	−0.57

Table 4. Initial composition of the different fluids, dissolved species in mol/L.

	Cement	Aquifer/Caprock	CO_2 Reservoir	CO_2-Reactive Solution
pH (-)	10.8	6.2	3.5	13.8
Ca^{2+}	1.30×10^{-2}	3.15×10^{-2}	3.10×10^{-2}	0.68
Mg^{2+}	1.69×10^{-8}	9.32×10^{-3}	9.16×10^{-3}	-
Na^{+}	1.0	0.98	0.98	1.03
K^{+}	-	8.62×10^{-3}	8.48×10^{-3}	-
H_4SiO_4	4.10×10^{-6}	8.57×10^{-4}	8.46×10^{-4}	-
HCO_3^{-}	-	8.29×10^{-3}	1.78	-
SO_4^{2-}	2.07×10^{-4}	3.25×10^{-2}	3.20×10^{-2}	-
Al^{3+}	4.14×10^{-4}	7.24×10^{-8}	7.12×10^{-8}	-
Cl^{-}	1.0	1.0	0.98	1.03

3. Results of CO_2 Leakage and Natural Sealing

3.1. CO_2 Leakage and Cement Reactions

The reactive transport simulations show upward flow of CO_2 through the microannulus. With the applied 20 bar overpressure, the flow rate of gaseous CO_2 through the microannulus is 2.1×10^{-5} kg/s. During upward flow, a fraction of the CO_2 gas dissolves into the cement and caprock pore water and diffuses horizontally into the cement and the caprock, thereby lowering the pH of the pore waters. Cement minerals react with the carbonized water and start to dissolve to buffer the pH. Similar to e.g., Kutchko et al. [6], we observe inward progression of reaction zones in the horizonal direction, which is limited by diffusion (Figure 2). The reaction zones are characterized by: portlandite dissolution and calcite formation, CSH dissolution with amorphous silica and calcite precipitation, monosulfoaluminate and hydrotalcite dissolution with dolomite (max. 0.003 volume fraction), gibbsite (max. 0.0025 volume fraction) and anhydrite (max. 0.009 volume fraction) precipitation. The further

up from the reservoir level, the less advanced the horizontal progression of these zones is, since the reactions only start as soon as the upward migration of the CO_2 reaches that level and the pH decreases. After 2 years of CO_2 leakage, approximately 1 cm of the cement just above reservoir level is affected by horizontal CO_2 diffusion and related reactions (Figure 2). The silicate minerals of the caprock do not show siginificant reactions within the simulated time. There is a minor increase of calcite in the caprock adjacent to the microannulus.

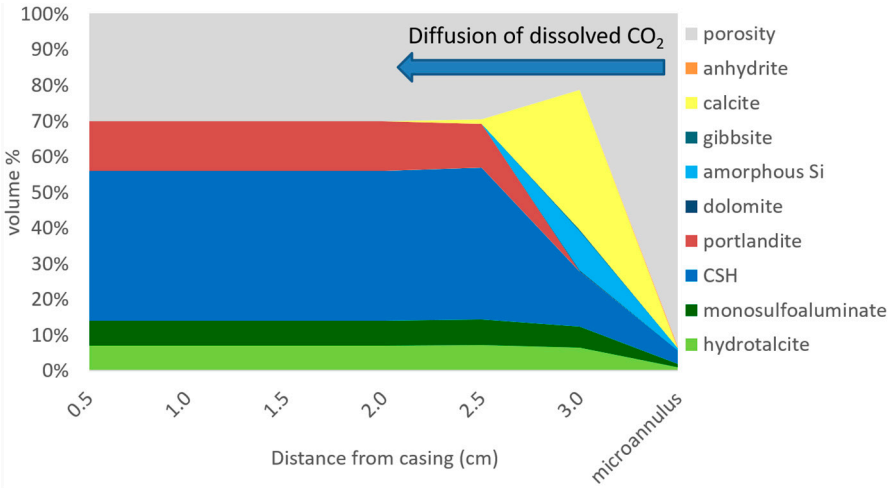

Figure 2. The cement mineralogy and porosity after two years of CO_2 leakage are plotted for a horizontal transect across the cement sheet and the microannulus, located just above the CO_2 reservoir. Cement reacts with CO_2 from the microannulus on the right. Note that, even though not well visible, small amounts of dolomite, anhydrite and gibbsite precipitate in the microannulus and cement.

After the CO_2 within the microannulus reached the top of the caprock, the pH is around 4.5 throughout the microannulus. In the cement affected by CO_2 interactions-adjacent to the microannulus-the pH is roughly 5 and in the unaltered cement nearly 11 (Figure 3). The pH decrease causes full dissolution of portlandite in the microannulus and adjacent cement cells and gradual dissolution of the other cement phases such as CSH, with decreasing amount of dissolution from the reservoir level upwards. As a result, secondary calcite is also highest at the level close to the reseroir (Figure 3). Within the microannulus calcite that precipitated is re-dissolved due to the low pH and flow conditions which allow quick removal of dissolved species. The permeability of the microannulus is predicted to increase from 1.3×10^{-12} m^2 to 1.9×10^{-12} m^2 after 2 years of CO_2 flow and corresponding cement alteration.

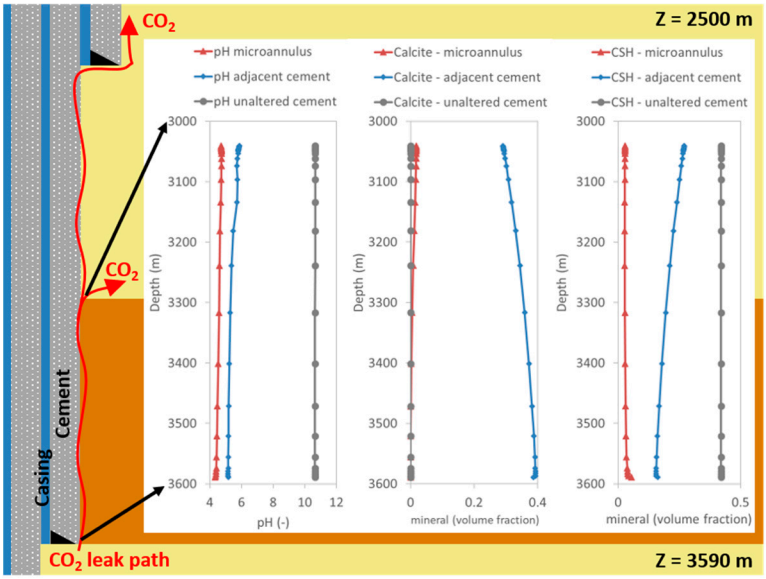

Figure 3. The background shows a schematic overview of the model with a cement sheet, the microannulus leak path and the adjacent formation rock. The pH, calcium silicate hydrate (CSH) content and calcite content after two years of CO_2 leakage are plotted for the lower part of the annulus adjacent to the caprock.

3.2. *Microannulus Leakage Versus Natural Sealing*

Four permeability values were selected to simulate different initial leakage rates and to assess the chemical processes within a leaking or self-sealing annulus. Results are discussed after half a year of leakage simulation. The different permeabilities yield different levels of gas saturation, with a higher gas saturation for a higher permeability (Figure 4a). For all scenarios, the flow of CO_2 and dissolution of CO_2 in the initially water saturated microannulus result in complete dissolution of portlandite within the microannulus—which was 10% cement filled—and subsequent precipitation of calcite (Figure 4b). Above the reservoir, re-dissolution of calcite can be observed. Only for the lowest permeability of 1×10^{-13} m^2, CO_2 gas does not reach the top of the caprock. This is due to natural sealing of the microannulus, with complete calcite clogging in the middle part of the microannulus. The front of calcite precipitation is characterised by a peak in calcium content (Figure 4c) and an increase in pH (Figure 4d). The permeability of the microannulus depends on the initial permeability and the dissolution and precipitation reactions. There is a high permeability near the reservoir where the calcite content is lowest (Figure 4e). The 1×10^{-11} and 5×10^{-11} m^2 scenarios show only little permeability change in the upper part of the microannulus due to portlandite dissolution and calcite precipitation. The initial permeability value 1×10^{-12} m^2 is more affected by calcite precipitation and the 1×10^{-13} m^2 scenario shows complete permeability impairment due to calcite clogging.

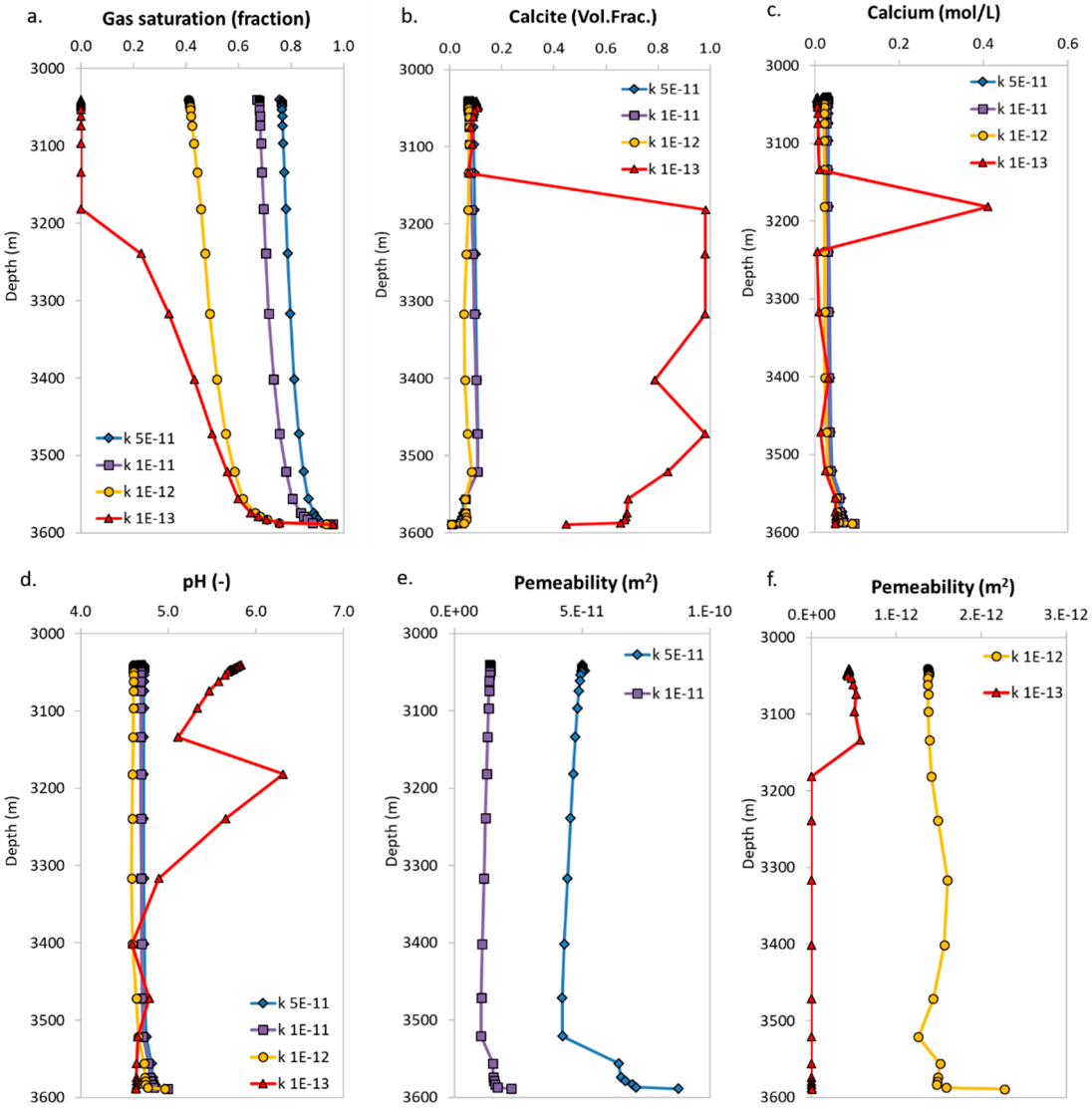

Figure 4. Simulation results along the microannulus for four different initial microannulus permeabilities showing: (**a**) gas saturation, (**b**) calcite volume fraction, (**c**) dissolved calcium, (**d**) pH, and (**e**,**f**) the permeability of the high and low initial permeability scenarios respectively.

4. Results of CO_2 Reactive Leakage Remediation

4.1. Injection of the CO_2-Reactive Solution with Different Injection Pressures

The 1×10^{-12} m^2 permeability scenario is selected to model initial leakage and subsequent leakage remediation. Upward CO_2 leakage through the microannulus was simulated for half a year before leakage remediation was applied. To remediate leakage, a CO_2-reactive solution (composition given in Table 4) was injected into the CO_2 containing microannulus. The solution is injected at a depth of 3048 m, which is 8 m below the top of the caprock. The CO_2-reactive, lime-saturated solution is injected in order to react with dissolved CO_2 to form calcite ($CaO + CO_2 - > CaCO_3$). To inject the CO_2-reactive solution in the model, we used a fixed pressure cell adjacent to the microannulus to allow for pressure-controlled injection, instead of defining a fixed injection rate. The sensitivity of leakage remediation to flow rates was asessed by variying the pressure of injection with 1, 5 and 10 bar overpressure for the microannulus pressure of 324 bar.

For all three injection pressures, the injection of the CO_2-reactive solution leads to an initial increase followed by an interruption of the upward CO_2 flow in the microannulus, but flow recovers (after $t = 0$ in Figure 5, showing the results of 5 bar overpressure injection). Calcite starts to precipitate

in the microannulus at the level where the CO_2-reactive solution is injected. Gradually the permeability of the microannulus reduces with a corresponding decrease of the CO_2 and water flow rate (Figure 5). The rate of solution injection reduces as well, since the permeability decreases and the pressure is fixed. Figure 6a shows the initial higher injection rate with a higher overpressure and the decrease of injection rate with time. The moment of complete flow impairment occurs at the time when the microannulus adjacent to the injection cell is nearly filled with calcite, reducing the permeability to zero (Figure 5). All overpressures yield complete calcite clogging (Figure 6b), but with differences in the development of calcite precipitation due to the differences in the balance of calcium and CO_2 supply. Within 10 days, all injection pressure scenarios predict clogging the microannulus with calcite precipitation, preventing further leakage of the CO_2.

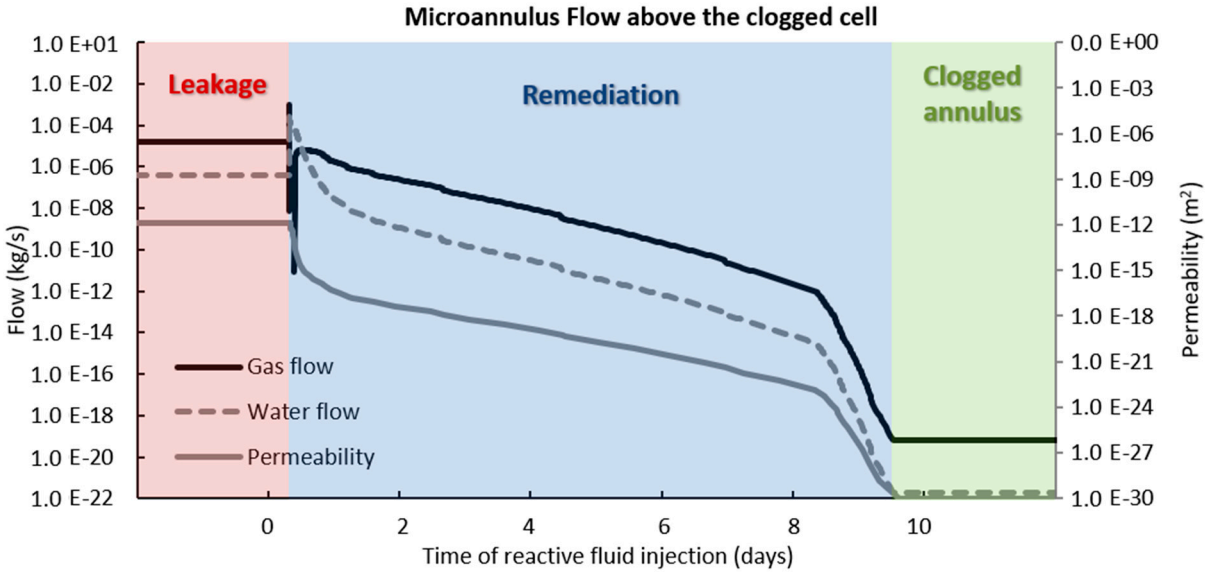

Figure 5. The development of CO_2 and water flow rate (left axis, logaritmic) and the permeability (right axis, logaritmic) in the microannulus at the level of injection of the CO_2-reactive solution. Results are from the 5 bar overpressure scenario. Data is plotted with time for the period around leakage remediation.

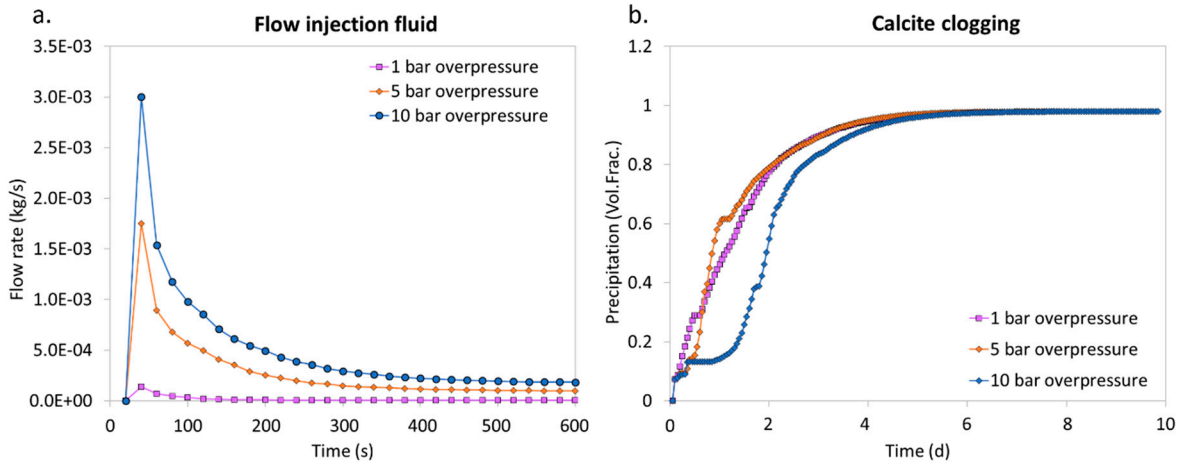

Figure 6. (**a**) The injection rate of the reactive solution for the three different injection pressures at the onset of the remediation procedure. (**b**) The evolution of calcite precipitation showing full clogging for all scenarios within the 10 days of leakage remediation.

4.2. Sensitivity to Porosity-Permeability Relation Input Parameters

The clogging process and specfically the calculation of the permeability based on the porosity development depends on highly uncertain porosity-permeability parameters [30]. A sensitivity study is performed reflecting the range in values for the critical porosity (φ_c) and power law (n) component as probed by Verma and Pruess [31] ($1 \leq n \leq 6$, $0.8\varphi \leq \varphi_c \leq 0.9\varphi$) and Xu et al. [35] ($4 \leq n \leq 13$, $0.88\varphi \leq \varphi_c \leq 0.94\varphi$). The initial leakage and subsequent remediation simulations (with a 1×10^{-12} m^2 permeability) were repeated for six combinations of 2 critical porosity values of 0.8 and 0.88 (80 and 88% reduction of the original porosity) with three different power law components of 2, 6 and 10.

The calcite plug formed using the different porosity-permeability relation input parameters is very similar (Figure 7). A peak of calcite precipitation is observed next to the cell from which the reactive solution is injected. Above this interval, the microannulus is only partially clogged due to calcite precipitation. The relative insensitivity of the characteristics of the calcite plug to the porosity-permeability relationship can be explained by the nature of the remediation process. The process is designed to inject the reactive solution up to full clogging, meaning that with all parameters a full permeability reduction will be simulated. There is a small difference in the calcite formed in the upper part of the plug, with the $0.88\varphi_c$–$2n$ model yielding the most precipitation and a combinitation of $0.8\varphi_c$ and $10n$ the least. The used porosity-permeability parameters do have a large impact on the predicted time that is required to achieve full clogging. The time it takes to perform the remediation method ranges from 7 to 113 days (Table 5). This indicates the importance of the porosity-permeability parameters for the prediction of the duration of the remediation procedure and for the asessment of the related costs and overall feasibility.

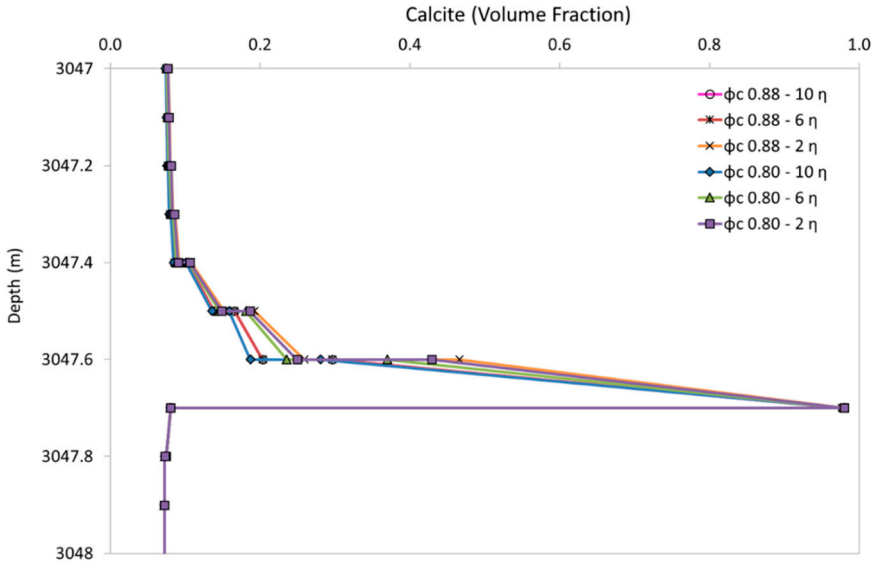

Figure 7. The calcite content for a 1 m section of the microannulus after leakage remediation, showing a peak adjacent to the level of reactive solution injection. The results are shown for six scenarios of different porosity-permeability relation input parameters.

Table 5. The predicted time of remediation up to full clogging of the microannulus.

Scenario (φ_c – η)	0.8–6	0.8–2	0.8–10	0.88–2	0.88–6	0.88–10
Remediation Time (d)	39	7	48	11	45	113

4.3. Stability of the Plug in Time

After the remediation procedure, the reactive transport simulation is continued for 1 year to assess the stability of the calcite plug with time. This allows for equilibration of the system and continuation of diffusion and possibly flow. To assess the stability of the plug and the chemical evolution within the

microannulus, two porosity-permeability scenarios were selected representing the most ($0.88\varphi_c - 2n$) and least calcite precipitation ($0.80\varphi_c - 10n$).

Throughout the microannulus, the pH remains around 4.6 in the post-remediation phase, indicating the wellbore environment is still acidic and is not buffered by the cement within the year after leakage remediation that was simulated. The caprock minerals show no significant reactions in this time period. The main observed process is the increase in calcite volume fraction throughout the microannulus (Figure 8a), the thin original plug is plotted for comparison. After the remediation method stops CO_2 leakage, the process of natural sealing becomes dominant throughout the micoannulus adjacent to caprock due to the absence of flow. This results in clogging by mainly calcite precipitation and minor amorphous silica precipitation. After one year of reactions following the remediation procedure, the $0.80\varphi_c$–$10n$ scenario yields full clogging of the microannulus (Figure 8a,b). The $0.88\varphi_c$–$2n$ scenario does have two sections of partial clogging, but full clogging of the rest of the microannulus (Figure 8b). The partial clogging above the original plug is due to absence of CO_2 which has been completely consumed, yielding a zero gas saturation (Figure 8c). The gas saturation is highest just below the plug and just above the CO_2 reservoir. The zero permeability of the plug continues to block the CO_2 flow and causes the gas saturation above the clogged level to decrease with time as CO_2 migrates and is consumed by reactions. The permeability impairment forms a pressure block, with the microannulus below the plug approaching the CO_2 reservoir pressure and the microannulus above the plug retaining hydrostatic pressure.

The two porosity-permeability scenarios both yield sigificant natural sealing after clogging by injection of the remediation fluid. This indicates that reduction of leakage due to the remediation procedure enhances the natural capability of the wellbore system to seal and form a barrier against future leakage.

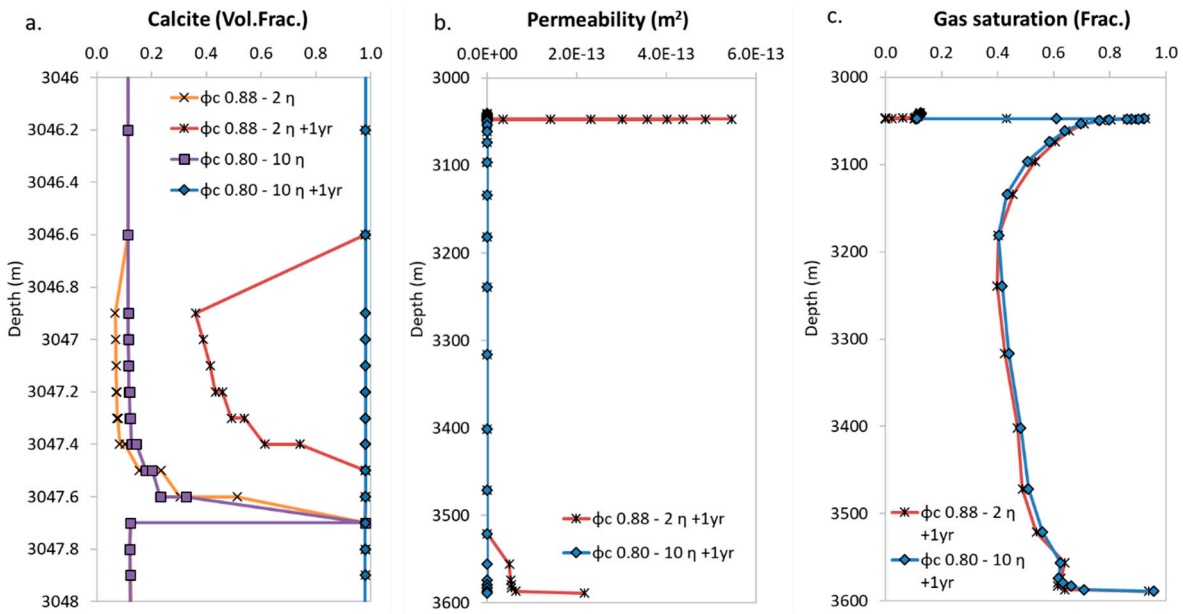

Figure 8. The development of the microannulus within 1 year after remediation. Results are shown for (**a**) calcite around the original plug, (**b**) permeability of the microannulus, and (**c**) gas saturation of the microannulus adjacent to the caprock.

5. Discussion and Conclusions

Despite the function of annular cement as a seal preventing oil, natural gas or stored CO_2 to migrate to aquifers or to the surface, wells are known to leak due to microannuli formed by processes such as cement shrinkage or pressure and temperature fluctuations [2,5]. The width of a microannulus formed tends to increase for larger temperature differences between the produced or injected fluid

and the rock formation, which is especially relevant for cold CO_2 injection [36]. The higher risk of microannulus formation during CO_2 injection combined with high abandonment pressures asks for an assessment of CO_2 microannulus leakage and methods for leakage remediation. Due to the high reactivity of cement with carbonated brine, the chemical processes are key. A field-scale wellbore model was developed which successfully incorporates CO_2 migration by two-phase flow through a microannulus and diffusion of dissolved CO_2 into the adjacent caprock and cement. This enables the simulation of the complex reactive transport processes of a storage system, including a storage reservoir, wellbore cement with a continuous microannulus from reservoir to caprock, and caprock overburden. Despite the large scale of the model, it was successful in predicting the well-known small-scale reaction characteristics as found in experimental and (small scale) modelling studies [6,8–12].

Previous simulations showed an initial critical CO_2 leakage velocity of 0.1×10^{-5} m/s below which calcium released from dissolving cement minerals can diffuse towards the microannulus where calcite forms which clogs the microannulus and prevents further flow [18]. For our models, a low enough leakage rate to facilitate natural sealing was achieved with an initial microannulus permeability of 1×10^{-13} m^2. The possibility for natural microannulus clogging at low leakage rates is similar to the self-sealing potential of fractures in cement as demonstrated by e.g., Huerta et al. [16]. They discussed the critical residence time for the CO_2 fluid to be present in a cement sample for a fracture to close. However, natural sealing is not solely dependent on the flow rate as determined by the systems permeability. Nonuniformity of the microannulus geometry can lead to local changes in flow velocity affecting the sealing process [19]. The specific chemistry of the cement and rock formations has a large impact, with, for example, a high potential for calcite forming in the microannulus when the host rock is a carbonate [17]. Previous modelling showed anhydrite clogging of the microannulus related to relatively high sulphate concentration in the formation water of the caprock [18], whereas the chemical characteristics of the cement and surrounding formation water in our model led to dominant calcite clogging. The thermodynamics and kinetics of the cement phases still pose uncertainty in the chemical processes in the microannulus [17]. Our kinetic parameters for CSH and silica may be considered conservative, yielding only minor amorphous silica in the microannulus. In addition, the uncertainty and variability in the reactive surface area of cement phases may further affect the predicted leaching of cement and natural sealing process. A dedicated uncertainty assessment with varying parameters for dissolution/precipitation kinetics and mineral reactive surface areas was out of the scope of this study but would be needed to assess the sensitivity to natural sealing of the microannulus.

For high leakage rates when natural sealing is not predicted to occur, the process of microannulus clogging can be induced by adding calcium to the system [22–24]. We injected a calcium-rich brine to react with the dissolved CO_2 in the microannulus, yielding a full permeability decrease due to calcite precipitation, as graphically represented in Figure 9. There are large uncertainties in the clogging process regarding the porosity-permeability relation of mineral precipitation in a microannulus. As discussed by Ito et al. [23] and Druhan et al. [24], the porosity-permeability relation is of utmost importance for predicting effective leakage remediation. However, compared to our previous numerical modelling study [22] in which we injected the CO_2-reactive solution in an aquifer above a caprock leak, leakage remediation in the microannulus was predicted to be more successful and far less sensitive to the porosity-permeability relation. This is due to the confined nature of a microannulus and the more difficult placement of a plug above a caprock leak path. In our study, the uncertainty of the porosity-permeability relation was primarily expressed in the time it takes for remediation and not in the success of remediation. A longer remediation time is related to the larger amount of mineral precipitation and porosity reduction that is required to achieve full permeability reduction when using a more conservative porosity-permeability relationship. Hence, accurate design of the remediation procedure requires additional data on the porosity-permeability behaviour of a microannulus. The previous study [22], indicated the significance of the leakage rate on the success of leakage remediation. The design of the remediation procedure would require knowledge on the actual leakage rate or a numerical sensitivity study on the possible range in initial microannulus permeability and resulting

leakage rate. With a higher initial leakage rate, injection of the reactive solution might require a higher injection pressure.

Permanent leakage remediation, considering long-term CO_2 storage, requires a chemically stable plug in the leak path. Our model results indicate that the formed calcite plug does not only remain stable, but that cessation of flow enables natural sealing in the microannulus at the level below the plug. The increase in sealing of the microannulus enhances the potential for intentional clogging as a remediation method. Future work could focus on the sensitivity of the intentional and subsequent natural clogging process to the chemistry of the CO_2 reactive solution and the cement and formation rock chemistry. The chemical nature of the plug is of less importance when subsequent natural sealing can take over the barrier function, even if a placed plug would degrade in time.

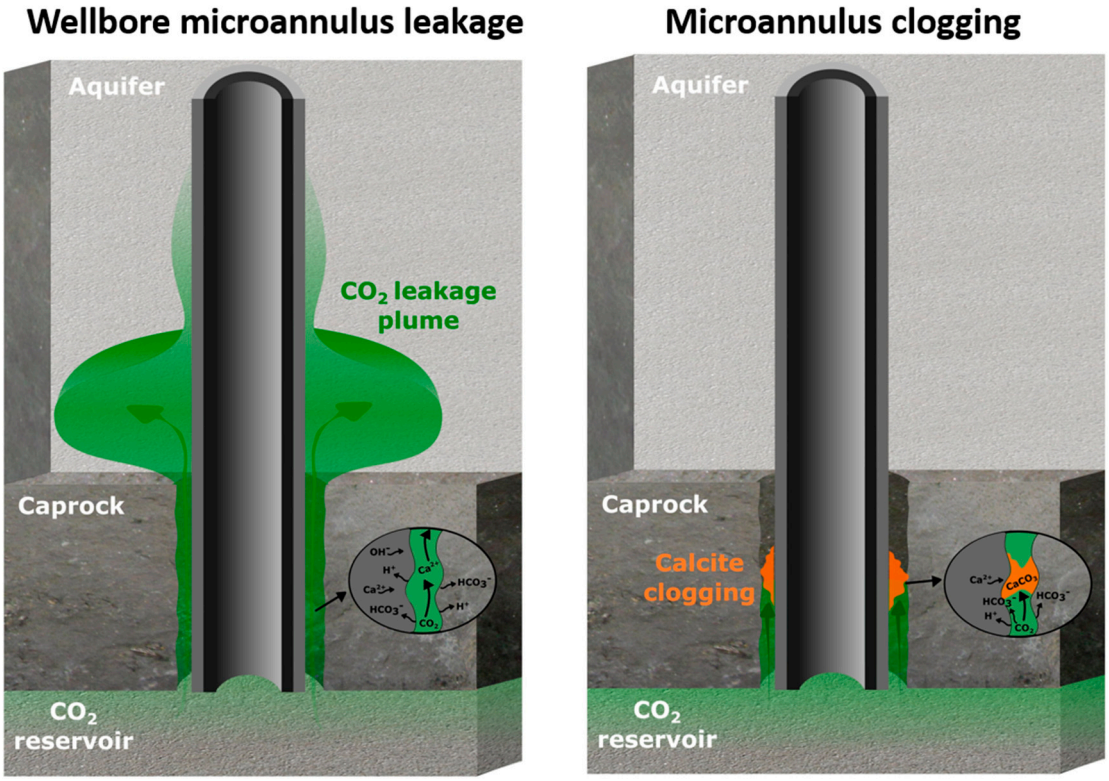

Figure 9. Graphical representation of the CO_2 leakage and CO_2-reactive remediation.

Author Contributions: Conceptualization, L.W. and M.K.; methodology, L.W. and M.K.; software, L.W. and M.K.; validation, L.W.; formal analysis, L.W.; investigation, L.W.; resources, L.W.; data curation, L.W.; writing—original draft preparation, L.W.; writing—review and editing, L.W. and M.K.; visualization, L.W.; supervision, L.W.; project administration, L.W.

Funding: This research received no external funding.

Conflicts of Interest: The authors declare no conflict of interest.

References

1. Metz, B.; Davidson, O.; Coninck, H.D.; Loos, M.; Meyer, L. (Eds.) *IPCC Special Report on Carbon Dioxide Capture and Storage*; Cambridge University Press: New York, NY, USA, 2005.
2. Dusseault, M.B.; Gray, M.N.; Nawrocki, P.A. Why oilwells leak: Cement behavior and long-term consequences. In Proceedings of the International Oil and Gas Conference and Exhibition in China, Beijing, China, 7–10 November 2000.
3. Bachu, S.; Bennion, D.B. Experimental assessment of brine and/or CO_2 leakage through well cement at reservoir conditions. *Int. J. Greenh. Gas Control* **2009**, *3*, 494–501. [CrossRef]

4. Carey, J.W.; Svec, R.; Grigg, R.; Zhang, J.; Crow, W. Experimental investigation of wellbore integrity and CO_2-brine flow along the casing-cement microannulus. *Int. J. Greenh. Gas Control* **2010**, *4*, 272–282. [CrossRef]
5. Gasda, S.E.; Bachu, S.; Celia, M.A. Spatial characterization of the location of potentially leaky wells penetrating a deep saline aquifer in a mature sedimentary basin. *Environ. Geol.* **2004**, *46*, 707–720. [CrossRef]
6. Kutchko, B.G.; Strazisar, B.R.; Dzombak, D.A.; Lowry, G.V.; Thauiow, N. Degradation of well cement by CO_2 under geologic sequestration conditions. *Environ. Sci. Technol.* **2007**, *41*, 4787–4792. [CrossRef]
7. Carey, J.W.; Wigand, M.; Chipera, S.J.; WoldeGabriel, G.; Pawar, R.; Lichtner, P.C.; Wehner, S.C.; Raines, M.A.; Guthrie, G.D., Jr. Analysis and performance of oil well cement with 30 years of CO_2 exposure from the SACROC Unit, West Texas, USA. *Int. J. Greenh. Gas Control* **2007**, *1*, 75–85. [CrossRef]
8. Huet, B.; Prevost, J.H.; Scherer, G.W. Quantitative reactive transport modeling of Portland cement in CO_2-saturated water. *Int. J. Greenh. Gas Control* **2010**, *4*, 561–574. [CrossRef]
9. Gherardi, F.; Audigane, P.; Gaucher, E.C. Predicting long-term geochemical alteration of wellbore cement in a generic geological CO_2 confinement site: Tackling a difficult reactive transport modeling challenge. *J. Hydrol.* **2012**, *420*, 340–359. [CrossRef]
10. Duguid, A.; Scherer, G.W. Degradation of oilwell cement due to exposure to carbonated brine. *Int. J. Greenh. Gas Control* **2010**, *4*, 546–560. [CrossRef]
11. Rimmelé, G.; Barlet-Gouédard, V.; Porcherie, O.; Goffé, B.; Brunet, F. Heterogeneous porosity distribution in Portland cement exposed to CO_2-rich fluids. *Cem. Concr. Res.* **2008**, *38*, 1038–1048. [CrossRef]
12. Barlet-Gouédard, V.; Rimmelé, G.; Porcherie, O.; Quisel, N.; Desroches, J. A solution against well cement degradation under CO_2 geological storage environment. *Int. J. Greenh. Gas Control* **2009**, *3*, 206–216. [CrossRef]
13. Temitope, A.; Gupta, I. A review of reactive transport modeling in wellbore integrity problems. *J. Petrol. Sci. Eng.* **2019**, *175*, 785–803.
14. Lea, F.M. The constitution of Portland cement. *Q. Rev. Chem. Soc.* **1949**, *3*, 82–93. [CrossRef]
15. Wasch, L.J.; Koenen, M.; Wollenweber, J.; Tambach, T.J. Sensitivity of chemical cement alteration—Modeling the effect of parameter uncertainty and varying subsurface conditions. *GHG S T* **2015**, *5*, 323–338. [CrossRef]
16. Huerta, N.J.; Hesse, M.A.; Bryant, S.L.; Strazisar, B.R.; Lopano, C. Reactive transport of CO_2-saturated water in a cement fracture: Application to wellbore leakage during geologic CO_2 storage. *Int. J. Greenh. Gas Control* **2016**, *44*, 276–289. [CrossRef]
17. Guthrie, G.D.; Pawar, R.J.; Carey, W.J.; Karra, S.; Harp, D.R.; Viswanathan, H.S. The mechanisms, dynamics, and implications of self-sealing and CO_2 resistance in wellbore cements. *Int. J. Greenh. Gas Control* **2018**, *75*, 162–179. [CrossRef]
18. Koenen, M.; Wasch, L.J. The Potential of CO_2 Leakage Along De-Bonded Cement-Rock Interface. In Proceedings of the 14th Greenhouse Gas Control Technologies Conference, Melbourne, Australia, 21–26 October 2018; Available online: https://ssrn.com/abstract=3365897 (accessed on 21 April 2019).
19. Wolterbeek, T.K.; Raoof, A. Meter-scale reactive transport modeling of CO_2-rich fluid flow along debonded wellbore casing-cement interfaces. *Environ. Sci. Technol.* **2018**, *52*, 3786–3795. [CrossRef]
20. Neele, F.; Grimstad, A.; Fleury, M.; Liebscher, A.; Korre, A.; Wilkinson, M. MiReCOL: Developing Corrective Measures for CO_2 Storage. *Energy Procedia* **2014**, *63*, 4658–4665. [CrossRef]
21. Pizzocolo, F.; Peters, E.; Loeve, D.; Hewson, C.W.; Wasch, L.; Brunner, L.J. Feasibility of Novel Techniques to Mitigate or Remedy CO_2 Leakage. In Proceedings of the SPE Europec featured at 79th EAGE Conference and Exhibition, Paris, France, 12–15 June 2017. [CrossRef]
22. Wasch, L.J.; Wollenweber, J.; Tambach, T.J. A novel concept for long-term CO_2 sealing by intentional salt clogging. *GHG S T* **2013**, *3*, 491–502.
23. Ito, T.; Xu, T.; Tanaka, H.; Taniuchi, Y.; Okamoto, A. Possibility to remedy CO_2 leakage from geological reservoir using CO_2 reactive grout. *Int. J. Greenh. Gas Control* **2014**, *20*, 310–323. [CrossRef]
24. Druhan, J.L.; Vialle, S.; Maher, K.; Benson, S. Numerical simulation of reactive barrier emplacement to control CO_2 migration. In *Carbon Dioxide Capture for Storage in Deep Geologic Formations—Results from the CO_2 Capture Project*; Gerdes, K.F., Ed.; CPL Press and BPCNAI: Thatcham, Berks, UK, 2015.
25. Wasch, L.J.; Wollenweber, J.; Neele, F.; Fleury, M. Mitigating CO_2 Leakage by Immobilizing CO_2 into Solid Reaction Products. *Energy Procedia* **2017**, *114*, 4214–4226. [CrossRef]

26. Xu, T.; Sonnenthal, E.; Spycher, N.; Pruess, K. TOUGHREACT—A simulation program for non-isothermal multiphase reactive geochemical transport in variably saturated geologic media: Applications to geothermal injectivity and CO_2 geological sequestration. *Computat. Geosci.* **2006**, *32*, 145–165. [CrossRef]
27. Pruess, K. *ECO2N: A TOUGH2 Fluid Property Module for Mixtures of Water, NaCl, and CO_2*; Lawrence Berkeley National Laboratory: Berkeley, CA, USA, 2005.
28. Blanc, P.H.; Lassin, A.; Piantone, P.; Azaroual, M.; Jacquement, N.; Fabbri, A.; Gaucher, E.C. Thermoddem: A geochemical database focused on low temperature water/rock interactions and waste materials. *Appl. Geochem.* **2012**, *27*, 2107–2116. [CrossRef]
29. Lasaga, A.C.; Soler, J.M.; Ganor, J.; Burch, T.E.; Nagy, K.L. Chemical weathering rate laws and global geochemical cycles. *Geochim. Cosmochim. Acta* **1994**, *58*, 2361–2386. [CrossRef]
30. Hommel, J.; Coltman, E.; Class, H. Porosity–Permeability Relations for Evolving Pore Space: A Review with a Focus on (Bio)geochemically Altered Porous Media. *Transp. Porous Med.* **2018**, *124*, 589–629. [CrossRef]
31. Verma, A.; Pruess, K. Thermohydrological conditions and silica redistribution near high-level nuclear wastes emplaced in saturated geological formations. *J. Geophys. Res.* **1988**, *93*, 1159–1173. [CrossRef]
32. Palandri, J.L.; Kharaka, Y.K. *A Compilation of Rate Parameters of Water-Mineral Interaction Kinetics for Application to Geochemical Modelling*; Open File Report; U.S. Geological Survey: Menlo Park, CA, USA, 2004.
33. Baur, I.; Keller, P.; Mavrocordatos, D.; Wehrli, B.; Johnson, C.A. Dissolution–precipitation behaviour of ettringite, monosulfate, and calcium silicate hydrate. *Cem. Concr. Res.* **2004**, *34*, 341–348. [CrossRef]
34. Marty, N.C.M.; Claret, F.; Lassin, A.; Tremosa, J.; Blanc, P.; Madé, B.; Giffaut, E.; Cochepin, B.; Tournassat, C. A database of dissolution and precipitation rates for clay-rocks minerals. *Appl. Geochem.* **2015**, *55*, 108–118. [CrossRef]
35. Xu, T.; Ontoy, Y.; Molling, P.; Spycher, N.; Parini, M.; Pruess, K. Reactive transport modeling of injection well scaling and acidizing at Tiwi field, Philippines. *Geothermics* **2004**, *33*, 477–491. [CrossRef]
36. Orlic, B.; Chitu, A.; Brunner, L.; Koenen, M.; Wollenweber, J.; Schreppers, G.-J. Numerical Investigations of Cement Interface Debonding for Assessing Well Integrity Risks. In Proceedings of the 52nd U.S. Rock Mechanics/Geomechanics Symposium, Seattle, WA, USA, 17–20 June 2018.